



**University of
Zurich**^{UZH}

**Zurich Open Repository and
Archive**

University of Zurich
University Library
Strickhofstrasse 39
CH-8057 Zurich
www.zora.uzh.ch

Year: 2008

MERIS Chl-a timeseries of Lake Constance 2003-2006

Odermatt, D ; Heege, T ; Nieke, J ; Kneubühler, M ; Itten, K I

DOI: <https://doi.org/10.1109/IGARSS.2008.4779855>

Posted at the Zurich Open Repository and Archive, University of Zurich
ZORA URL: <https://doi.org/10.5167/uzh-4012>
Conference or Workshop Item

Originally published at:

Odermatt, D; Heege, T; Nieke, J; Kneubühler, M; Itten, K I (2008). MERIS Chl-a timeseries of Lake Constance 2003-2006. In: 2008 IEEE International Geoscience Remote Sensing Symposium, Boston, US, 6 July 2008 - 11 July 2008, 846-849.

DOI: <https://doi.org/10.1109/IGARSS.2008.4779855>

MERIS CHL-A TIMESERIES OF LAKE CONSTANCE 2003-2006

Daniel Odermatt¹, Thomas Heege², Jens Nieke³, Mathias Kneubühler¹ and Klaus Itten¹

1 Remote Sensing Laboratories (RSL), Zurich, Switzerland; daniel.odermatt@geo.uzh.ch

2 EOMAP GmbH & Co. KG, Gilching, Germany; heege@eomap.de

3 ESA/ESTEC, Noordwijk, Netherlands; jens.nieke@esa.int

ABSTRACT

A physically based water constituent retrieval algorithm is used for the automatic processing of MERIS level 1B full resolution data. The algorithm requires several input variables for individual optimization with different sensors (i.e. channel calibration and weighting), aquatic regions (i.e. specific inherent optical properties) or atmospheric conditions (i.e. Aerosol models). The optical properties are derived from optical in situ measurements during concurrent MERIS data acquisition on 20 April 2007. Remaining parameters are iteratively optimized for best performance with 21 MERIS datasets of Lake Constance in the years 2003-2005, and validated with 11 datasets in 2006. Operational water quality sampling measurements acquired by local authorities serve as reference.

Index Terms—Inland water, chlorophyll, monitoring, operationalization

1. INTRODUCTION

Monitoring of water quality ensures the sustainable use of water and allows tracking the effects of anthropogenic influences. In the early 1990s, analytical methods applied to high spectral resolution airborne scanner data were found to bear the potential to overcome the spatial limitations of conventional methods for inland quality monitoring [1]. MERIS provides a nominal revisit time of 2-3 days at mid latitudes at 300 m spatial resolution, and is therefore appropriate for water quality monitoring of the largest prealpine lakes. However, especially atmospheric correction remains a critical issue with current applications [2].

MIP (Modular Inversion and Processing System) algorithms are based on the minimization of the difference between satellite measured and modeled spectra [3]. For this work, MIP is made applicable for automatic processing by optimizing a single, lake specific parameterisation for MERIS data of Lake Constance.

Lake Constance is the second largest lake in Western Europe, covering an area of 535 km² shared by Austria, Germany and Switzerland. It's located at 395 m a.s.l., its

average and maximum depth are 101 m and 253 m, respectively. 15% of its area is shallow water of less than 10 m depth. Anthropogenic eutrophication of Lake Constance reached a peak in the late 1970s, followed by 20 years of steady reoligotrophication [4]. Bi-weekly water quality monitoring measurements are carried out by IfS (Lake Research Institute), on behalf of IGKB (International Commission for the Protection of Lake Constance). They display up to 12 µg/l during spring blooms, and average concentrations of 1 µg/l in winter and 3-5 µg/l in summer and autumn [5].

2. DATA

2.1. MERIS imagery

The total 33 MERIS level 1B full resolution data used in this study are free of clouds and sun glint. Only subsets of and quarter scenes are processed. Extraction, conversion, processing and illustration are fully automatic [6]. MERIS meta data and quality flags are included in the processing, but the removal of images affected by sun glint was done manually, since MERIS' sun glint warning flags are not applied for inland waters.

2.2. Field campaign data

During MERIS' data acquisition on 20 April 2007 (Figure 1), subsurface irradiance reflectance R_r was measured in four sites. The measurements were carried out with two RAMSES AAC instruments [7] from DLR onboard a research vessel of IfS.

Each dataset is an average of more than 20 5 s sampling intervals, spectrally binned to 70 channels between 350 and 700 nm, at intervals of 5 nm. Outliers were manually removed, but some instrument noise persists, especially at 600-700 nm in the data of site B (Figure 2). Direct reference measurements of constituents were taken from water samples. Chlorophyll-a (chl-a) was measured with a fluorometer probe, which is cross-calibrated with the HPLC measurements by IfS. Suspended matter (sm) was filtered with a 1 µm glass fiber filter, as the sum of organic and

anorganic matter. Laboratory measurements of Gelbstoff (y) display unexpected offset changes at constant spectral shapes. The inverted RAMSES measurements were thus taken as reference.



Figure 1: 20 April 2007 MERIS true color composite of Lake Constance. FU, A-C indicate in situ measurements (Figure 2). Geometric correction was not applied.

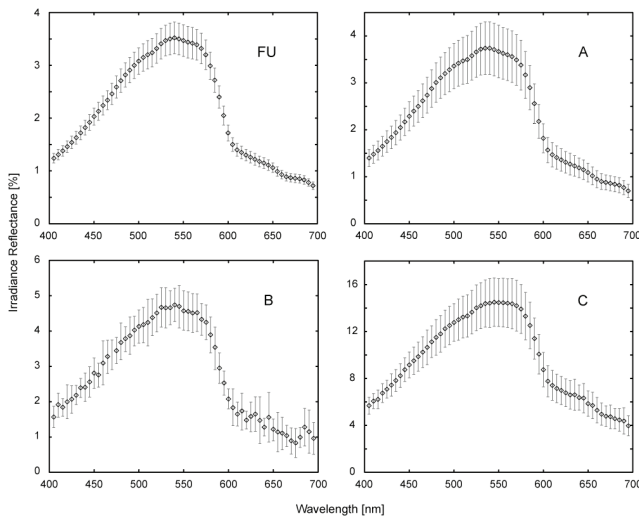


Figure 2: RAMSES data of 20 April 2007, corresponding to the sites FU and A-C in Figure 1.

2.3. Chl-a reference data

In situ chl-a measurements carried out by Ifs are sampled at the site Fischbach-Uttwil (FU, Figure 1, 47.62N / 9.37E), in approximately bi-weekly intervals. FU is located in the lake's deepest area and is further off shore than the other sites. The method used for chl-a determination is HPLC (High Performance Liquid Chromatography) [8]. 21 measurements within 3 days of MERIS data acquisition were used to build a training dataset for the years 2003-2005. 7 concurring validation data pairs of 2006 were complemented with 4 MERIS images for which the chl-a data had to be interpolated between two dates of low variability.

3. METHODS

For atmospheric correction, MIP uses a look up table (LUT), which was simulated with a coupled, plane-parallel atmosphere-water model and the finite element method (FEM) [9]. The module relates at-sensor radiances L_s to aerosol optical thicknesses (AOT) of either continental, maritime or rural aerosol type, observation geometry, wavelength and the subsurface radiance reflectance R_L^- , which is mainly due to backscattering on suspended matter (sm) at large wavelengths. The resulting AOT map is used to retrieve the angularly dependent subsurface radiance reflectance R_L^- for channels 1-8 from the same LUT. Another LUT is used to account for the directionality of the underwater light field, thus to convert R_L^- to the angularly independent subsurface irradiance reflectances R^- . It consists of Q-factors for varying wavelengths, observation geometries and water constituent concentrations, and is applied to R_L^- according to Equation 1:

$$R^- = R_L^-(\Delta\phi, \theta_{obs}, \theta_{sun}) \pi / Q(\Delta\phi, \theta_{obs}, \theta_{sun}) \quad (\text{Eq. 1})$$

The inherent optical properties (IOP) of water are related to R^- through Equation 2 [10], where f is parameterized as a function of μ [11], and μ is calculated for $z = 0$ m as a function of a , b , and the mean cosine of the incident light field [12].

$$R^- = f b_b / (a + b_b) \quad (\text{Eq. 2})$$

The coefficients x_i for absorption ($x=a$), scattering ($x=b$) and backscattering ($x=b_b$) of pure water ($i=w$), chlorophyll-a ($i=chl-a$), suspended matter ($i=sm$), and gelbstoff absorption ($i=y$) are calculated by Equation 3.

$$x = x_w + x_{chl-a}P + x_{sm}SM + x_y y \quad (\text{Eq. 3})$$

The inversion of subsurface irradiance reflectance R^- to the coefficients x_i is accomplished by means of a downhill simplex algorithm [13]. Maps of chl-a and sm concentration, y absorption (400 nm) and AOT (550 nm) are post processed with a selective, residual based filter. A more detailed description of the processing procedure and its parameterization is given in [6].

4. RESULTS

The chl-a concentrations of RAMSES and MERIS inversion and fluorometer measurements of 20 April 2007 reveal slightly higher values for RAMSES in sites A-C (Table 1). In FU, the RAMSES inversion produced higher y absorption than in the other sites, but outputs a relatively low chl-a concentration. These two parameters can act as substitutes in the inversion and therefore cause certain discrepancies. Another uncertainty lies in the high spatio-temporal variation on the border of the plume in the center of the main basin, which is visible in Figure 3 and Figure 4, and might have changed during the 3 hours of reference data acquisition. The sm concentrations agree better, with only the RAMSES estimate of site C revealing a larger offset. Y

estimates by MERIS are impossible due to low reliability of the calculated R^2 in channels 1 and 2, especially with difficult atmospheric conditions such as on 20 April 2007.

Table 1: 20 April 2007 reference measurements (lab), inversion results for RAMSES (ram, Figure 2) and MERIS (mer). MERIS acquisition was at 9:46 UTC.

Site	UTC	chl-a [mg/m^3]			sm [g/m^3]		
		lab	ram	mer	lab	ram	mer
FU	8:20	0.8	1.1	1.4	0.6	0.6	0.8
A	9:25	1.1	1.9	1.1	0.8	0.7	0.7
B	10:20	1.1	1.3	0.9	1.0	0.9	0.7
C	11:05	3.6	4.9	3.2	2.3	3.9	1.7

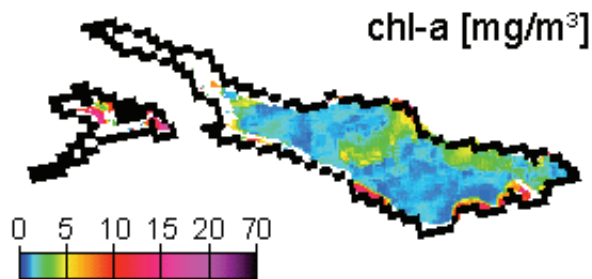


Figure 3: Chl-a map for 20 April 2007.

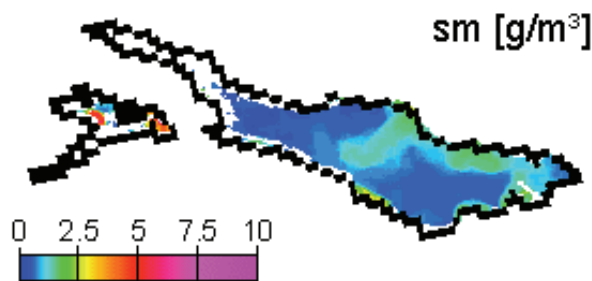


Figure 4: Sm map for 20 April 2007.

21 datasets of the years 2003-2005 were used for iterative training of water constituent retrieval channel weighting factors (Figure 5). Furthermore, we optimized model/sensor cross calibration factors for each channel, up to 3% of the original sensor radiances [6]. A maximum correlation coefficient of 0.79 is achieved by this procedure. However, the HPLC chl-a reference data of 29 March 2004 contradicts simultaneous fluorometer measurements, and the MERIS image of 18 April 2005 reveals a strong spatial variation of chl-a concentrations, with more similar values retrieved for adjacent pixels. If these two data pairs are excluded, the correlation coefficient increases to 0.94.

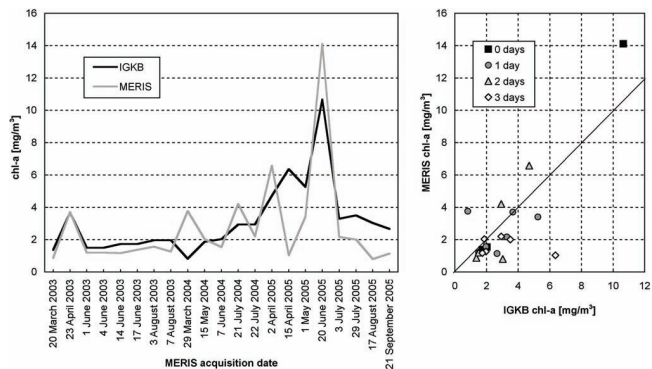


Figure 5: Correlation of 21 training data pairs for chl-a in the site FU, 2003-2005. The number of days between data acquisition are indicated in the figure on the right.

11 datasets acquired in 2006 were processed with the weighting and recalibration optimized for 2003-2005 data. The agreement is good for the first 8 datasets from March to August, correlating at a coefficient of 0.89, and representing the spring bloom, low chl-a in summer and an increase in August. However, an extraordinary increase in autumn is found in IGKB data, which is not found in MERIS imagery, leading to a low overall correlation (Figure 6).

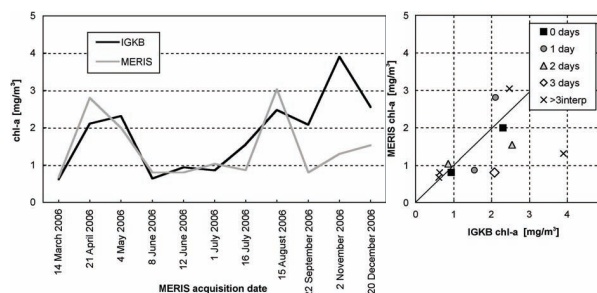


Figure 6: Correlation of 11 chl-a validation data pairs for chl-a in the site FU, 2006. The number of days between data acquisition and interpolated reference data pairs are indicated in the figure on the right.

The late autumn chl-a maximum might partly be caused by extraordinary SIOP [6]. However, a closer investigation of the chl-a output for 2 November 2006 reveals another issue. The image based AOT estimate from channel 14 is between 0.05 and 0.06 m^{-1} . This leads to very low reflectances especially in channels 6-8 (Figure 8, left). Pink areas in Figure 7 indicate maximum chl-a concentrations due to approximation of these channels by the algorithm. In the areas of blue color, channels 2-5 overrule channels 6-8 in the curve fitting, leading to lower but not necessarily more adequate results. However, when AOT is manually lowered to 0.01 m^{-1} , the atmospheric correction output spectrum is much higher in reflectance and its shape is much more similar to the modeled spectrum (Figure 8, right). Such low AOT might be unrealistic for mid latitude rural areas, but it is a strong indication for an inadequate calculation of AOT in visible wavelength's channels from NIR channel 14.

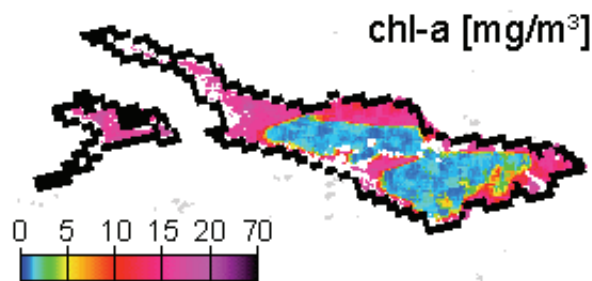


Figure 7: Chl-a concentration map for 2 November 2006. Pink color represents threshold concentrations allowed by the algorithm, indicating erroneous processing.

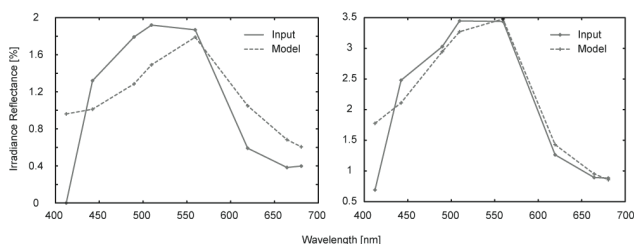


Figure 8: Input/model fits representing the pink area in Figure 7 after atmospheric correction with image retrieved AOT (550 nm)=0.05 m⁻¹ (left) and manually set AOT (550 nm)=0.01 m⁻¹ (right).

11. REFERENCES

- [1] Dekker, A., T. J. Malthus and H. J. Hoogenboom, "The remote sensing of inland water quality", *Advances in Environmental Remote Sensing*, Eds. F. M. Danson, S. E. Plumer, Wiley & Sons, New York, pp. 123-142, 1995.
- [2] Gege, P., and S. Plattner, "MERIS validation activities at Lake Constance in 2003", *Proc. of the MERIS User Workshop*, Frascati (Italy), 10-13 November 2003.
- [3] Heege, T., and J. Fischer, "Mapping of water constituents in Lake Constance using multispectral airborne scanner data and a physically based processing scheme", *Can. J. Remote Sensing* 30/1, Canadian Remote Sensing Society, Ottawa (Canada), pp. 77-86, 2004.
- [4] Liechti, P. *Der Zustand der Seen in der Schweiz*, BUWAL Schriftenreihe Umwelt, Nr. 237, 159 p., 1994 (in German).
- [5] Mürle, U., J. Ortlepp, P. Rey, *Der Bodensee - Zustand, Fakten, Perspektiven*, IGKB, 185 p., 2004 (in German).
- [6] Odermatt, D., T. Heege, J. Nieke, M. Kneubühler, K. Itten, Water quality monitoring for Lake Constance with a physically based algorithm for MERIS data, Manuscript submitted for publication.
- [7] TriOS Mess- und Datentechnik GmbH, *RAMSES Hyperspectral Radiometer Manual*, Rel. 1.0, 27 p., 2004.
- [8] Utermöhl, H., "Zur Vervollkommnung der quantitativen Phytoplankton-Methodik", *Mitt. Int. Ver. Theor. Angew. Limnol.*, 38 p., 1958 (in German).
- [9] Kiselev, V., B. Bulgarelli, Reflection of light from a rough water surface in numerical methods for solving the radiative transfer equation, *J. Quant. Spectrosc. Radiat. Transfer*, 85, pp. 419-435, 2004.
- [10] Gordon, H. R., O. B. Brown, O. B., M. M. Jacobs, Computed relationships between the inherent and apparent optical properties of a flat homogeneous ocean, *Appl. Opt.*, 14/2, pp. 417-427, 1975.
- [11] Kirk, J. T. O, Volume scattering function, average cosines, and the underwater light field, *Limnol. Oceanogr.*, 36/3, pp. 455-467, 1991.
- [12] Bannister, T. T, Model of the mean cosine of underwater radiance and estimation of underwater scalar irradiance, *Limnol. Oceanogr.*, 37/4, pp. 773-780, 1992.
- [13] Nelder, J. A., R. Mead, A simplex method for function minimization, *Comput. J.*, 7, pp. 308-313, 1965.